



Evidence for two upper mantle sources driving volcanism in Central Kamchatka

Alex Nikulin^{a,*}, Vadim Levin^a, Michael Carr^a, Claude Herzberg^a, Michael West^b

^a Rutgers University, Department of Earth and Planetary Sciences, 610 Taylor Rd., Piscataway, NJ 08854, United States

^b University of Alaska, Fairbanks, Geophysical Institute, 903 Koyukuk Dr., Fairbanks, AK 99775, United States

ARTICLE INFO

Article history:

Received 16 June 2011

Received in revised form 23 December 2011

Accepted 28 December 2011

Available online xxxx

Editor: P. Shearer

Keywords:

seismology
volcanology
arc volcanism
subduction zones

ABSTRACT

Volcanoes of the Central Kamchatka Depression (CKD) form the most active arc volcano system in the world. Volcanoes of the CKD are positioned ~170 km above the subducting Pacific Plate, in excess of the typical global value of ~100 km for arc volcanism. We present results of a combined geophysical and petrological study of the main volcanic center in the CKD, and argue for the presence of a second contributing melt source within the mantle wedge. This region of melt generation is separate from the fluid fluxed region above the subducting Pacific Plate; it may explain the presence of the active CKD arc in its current location.

Results of receiver function imaging of the upper mantle beneath CKD reveal a distinct area of low velocities at approximately 110 km depth that is clearly distinct from the crust of the subducting Pacific Plate. Results of petrological modeling suggest presence of pyroxenite source melt contribution to CKD lavas, alongside previously described peridotite source melts. We contend that our results advance the notion that melting at two separate sources, rather than the simple flux-induced melting within the mantle wedge, drives volcanoes of the CKD.

© 2012 Elsevier B.V. All rights reserved.

1. Introduction

The Pacific Plate is actively subducting beneath the Kamchatka peninsula at about 80–100 mm/yr. The subduction direction is about 310° relative to a fixed overriding plate and the angle of subduction decreases from 50° beneath the southern tip of Kamchatka to 35° at the northern termination of the Benioff zone (Gorbatov et al., 1997; Syracuse and Abers, 2006). Volcanic arcs vary in their positions relative to the Kamchatka trench and may be grouped into three distinct clusters (Fig. 1) – the nearly extinct Sredinny Range (SR), the active Eastern Volcanic Front (EVF) and the very active Central Kamchatka Depression (CKD). Geochemically, lavas of active EVF and CKD volcanoes fall within a common range of global arc volcanism, showing relative enrichment in large ion lithophile elements (Rb, Ba, K, Pb, Sr, Li, and B) with respect to high field strength elements (Nb, Zr and Ti) (Avdeiko et al., 2007; Ishikawa et al., 2001; Volynets, 1994).

The focus of this study is the most active volcanic cluster of the CKD – the Klyuchevskoy Group (KG). The 4750 m high Klyuchevskoy Volcano (KV) is the most prominent volcano of this cluster with a mean eruptive rate of 1 m³/s over the last 10 kyr (Fedotov et al., 1987). It produces lavas of basaltic to basaltic-andesitic composition. Aside from being the largest volcano in the KG, it is also the youngest,

with most of the edifice formed within the last 7000 yrs according to stratigraphy and ¹⁴C radiometric dating (Braitseva et al., 1995). The position of the subducting slab beneath the KG, estimated at 150–180 km (e.g., Avdeiko et al., 2007; Gorbatov et al., 1997), exceeds the typical depth to the subducting plate beneath arc volcanoes, estimated at ~110 km, (e.g. 108 ± 14 km (Tatsumi and Eggins, 1995); 112 ± 19 km (Tatsumi, 1986) and 124 ± 38 km (Gill, 1981)).

Compared to most Kamchatka volcanoes, the geochemistry of KV eruptive products indicates more complex magma evolution, with some geochemical patterns separating the KV from other arc volcanoes. In particular, KV erupts both high-MgO basalts and high-Al₂O₃ basaltic andesites (Khubunaya et al., 1994), with the most recent studies indicating that both lava types erupted coevally in the past (Khubunaya et al., 2007). Using CO₂ laser fluorination analysis of individual and bulk olivine phenocrysts and their host glass from KV basalts, Auer et al. (2009) inferred high δ¹⁸O values in conjunction with elevated concentrations of H₂O, which they interpreted to indicate a high fluid flux component.

Multiple geodynamic models were proposed to explain the voluminous volcanism in the CKD. In many of them the large extent of partial melting in the mantle wedge beneath the CKD is driven by subduction of the Hawaii–Emperor Seamount (HES) chain. In this model fluid release from the thick, highly hydrated HES crust triggers extensive flux-induced melting in the mantle (Dorendorf et al., 2000; Kersting and Arculus, 1994; Volynets, 1994). Yogodzinski et al. (2001) first argued for the mantle flow around the corner of the Kamchatka–Aleutian junction, while in the scenario of Levin et al. (2002) a portion of the subducting slab has separated and descended

* Corresponding author. Tel.: +1 347 609 8533.

E-mail address: anikulin@rutgers.edu (A. Nikulin).

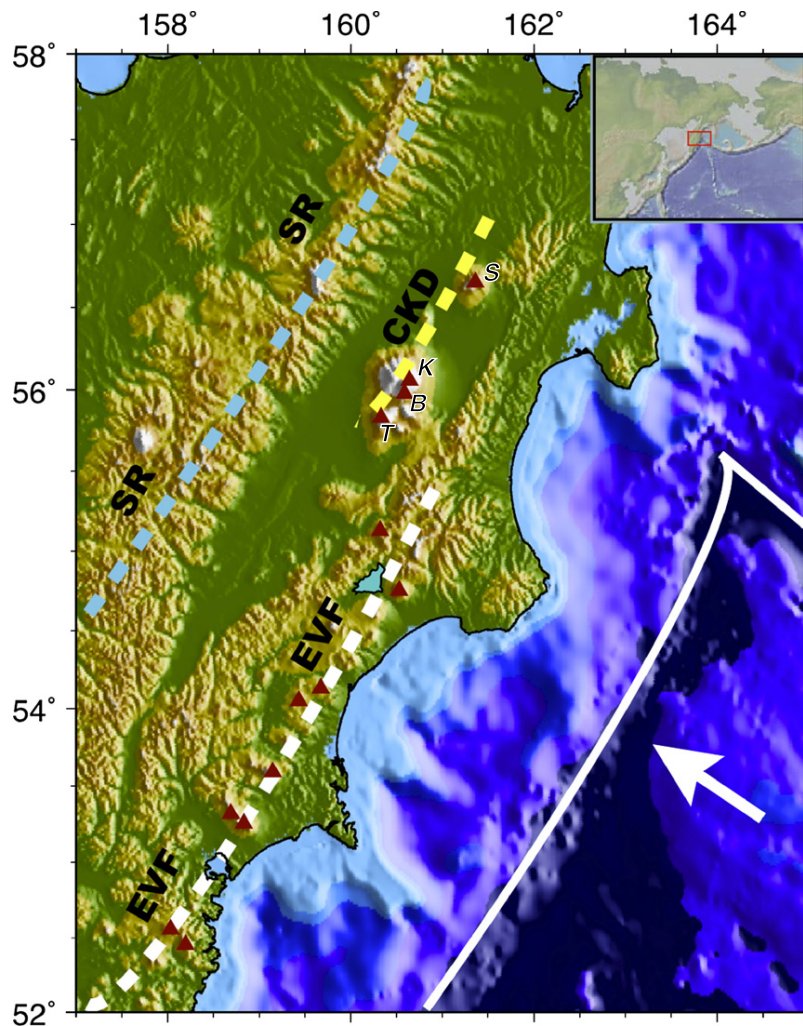


Fig. 1. Overview map of major geological structures of the Kamchatka subduction zone. Subduction direction is indicated by the white arrow, volcanoes are labeled with red triangles, dashed lines indicate the orientation of the three main volcanic clusters of Kamchatka. Letters indicate volcano names of Central Kamchatka (K – Klyuchevskoy, T – Tolbachik, B – Bezymianny, S – Shiveluch).

into the mantle during the Pliocene, opening a pathway for the upwelling of hot asthenospheric material.

The origin of geochemical variation recorded in the lavas of the KG continues to be contested. To explain the simultaneous production of high-MgO basalts and high- Al_2O_3 basaltic andesites, Kersting and Arculus (1994) and Ozerov (2000) proposed progressive tapping, recharge and fractionation of high-MgO parental magmas as a way to generate high- Al_2O_3 basaltic andesites. Ariskin et al. (1995) invoked a model involving polybaric fractionation under hydrous conditions. More recently, Portnyagin and Manea (2008) argued that the geochemistry of CKD lavas can be attributed to variations in the thermal conditions of magma generation beneath the region, which is in turn related to the geometry of the subducting slab.

We present new geophysical and petrological observations that suggest a model with two separate melt generation regions in the mantle wedge of the KG. The first contributing source is the subduction fluid induced flux melting vertically adjacent to the surface of the subducting Pacific Plate. The second source is positioned within the mantle wedge at a depth of ~100 km and may be related to pyroxenite melting. Their simultaneous activity may be able to better explain the unusual geographical position of the KG cluster; its elevated level of volcanic activity, and the geochemical variability recorded in lavas of the KG.

1.1. Receiver function imaging

Receiver functions (RFs) describe P-to-S converted waves generated at each interface encountered by the teleseismic P wave (Phinney, 1964; Vinnik, 1977). RF analysis has been successfully used to detect velocity contrasts associated with subducted slabs (Ferris et al., 2003; Langston, 1981; Nikulin et al., 2009; Park et al., 2004). Nikulin et al. (2010) employed this method to probe the mantle beneath the CKD using a dataset recorded by three broadband stations deployed around the Bezymianny volcano from 2007 to 2009. Results of the present paper are based on additional data recorded by the same three stations in 2010 and a modified algorithm to convert time-domain RF data to depth.

We compute receiver functions for “beams” formed by grouping observed earthquakes on the basis of their location. A center and the ranges of back azimuths and epicentral distances define each beam. Receiver functions from individual sources within a beam are combined using the multitaper spectral correlation algorithm of Park and Levin (2000). A resulting receiver function is associated with a ray path connecting the center of the beam and the station. We use a set of “beams” overlapping in both back azimuth and epicentral distance by 50% (i.e. the distance between beam centers is equal to half of the beam width). Our method resembles that employed by Bostock (1999), but adds spatial overlap of the beams

in the manner previously used either in back azimuth or epicentral distance in our studies utilizing MTC technique (e.g., Nikulin et al., 2009, 2010). The resulting beam-formed RFs are subsequently converted from time to depth using a seismic velocity model for Kamchatka that includes AK-135 model of Kennett et al. (1995) for the bulk mantle, the model of Nizkous et al. (2006) for the uppermost mantle, and that of Shapiro et al. (2000) for the crust. We build a database of P-S conversion points beneath the central point of the three stations (lat: 160.63, lon: 55.96) relying on the TauP algorithm (Crotwell et al., 1999). For a depth range of 0–200 km, we calculate geographical coordinates and hypothetical P-S delay times for pierce points every 5 km along the ray. We determine this information for rays from a grid of sources (that is, beam centers) located every 15° in back azimuth, and every 10° in epicentral distance range 20°–90°. In all, we calculate geographical coordinates of 3840 hypothetical pierce points for 96 hypothetical beams for the central point. We compound matched traces as a three-dimensional volume of 6607 conversion points with assigned geographical coordinates, depths and RF amplitudes. The correlation between time-domain and depth domain observations is illustrated in Fig. 2 (panels a and b).

The result of RF migration projects P-S converted pulses to the depths where they originate, allowing us to construct images of impedance contrasts within the volume beneath our stations. We present our findings in Fig. 3 as a volume of migrated receiver functions computed with an upper frequency limit of 0.375 Hz and projected onto vertical planes along and orthogonal to the vector of the Pacific Plate motion. Individual RF values for specific P-S conversion points at depth are first projected onto the vertical plane, and then averaged within rectangular blocks 4 × 4 km in size. We color RF amplitudes using the same scheme as in Nikulin et al. (2010) – positive pulses are blue, negative are red. A positive (blue) P-SV conversion implies an increase of impedance with depth, while a negative (red) pulse indicates a decrease of impedance with depth (see Fig. 2c). Our cross sections are centered on Bezymianny volcano.

Seismicity recorded by the Kamchatka Branch of Geophysical Service (Russian Academy of Sciences) with $M_L=5$ and epicenters within 25 km of the cross sections is projected in Fig. 3, and shows three distinct clusters: crustal earthquakes beneath the volcanoes, a well-delineated Wadati–Benioff zone, and more diffuse deeper seismicity that may be within the subducting Pacific Plate.

In our image, the dipping zone of seismicity clearly correlates with a region of distinct positive RF pulses. This indicates a downward increase in impedance, which we interpret as the crust–mantle boundary of the subducting Pacific Plate. Its position matches previously proposed depth of ~170 km beneath the KG (Avdeiko et al., 2007; Gorbatov et al., 1997; Portnyagin and

Manea, 2008) and can be seen as initial verification of our imaging procedures.

Based on results of past studies we expect the RF signature of the Moho transition beneath the CKD to be very faint. Both tomographic (Gorbatov et al., 1997) and active source deep sounding studies (Balesta et al., 1977) indicate a gradational change in seismic wave speed between the crust and upper mantle. We observe a faint blue feature, corresponding to a fast-to-slow boundary at a depth of approximately 30 km beneath the recorders. This weakly imaged contrast corresponds to the phase at ~3.7 s (see Fig. 2a) and likely marks the gradual contact between the upper mantle and crust beneath Central Kamchatka.

Our results indicate that the velocity structure beneath the KG is dominated by the anomalous feature observed in the upper mantle at ~100 km depth. This feature is marked by velocity contrast more intense than those that can be correlated to the subducting plate signature or the faint Moho, and is clearly separated from both in the image (Fig. 3). In the cross-section C–D the anomaly appears to dip to the south. The exact orientation of the feature in the image is likely affected by our imaging geometry, with tight concentration of observation points in one place. The P-SV mode converted waves that form receiver function time series are registered at times relative to the arrival of their parent P waves. If mode conversion takes place at an inclined interface, pierce points for P and P-SV waves are not coincident leading to directional dependence of the delay (see lines in Fig. 2a). In studies where observations are available over a broad area this effect is mitigated by crossing rays for different sites. We model the true geometry of the feature as dipping ~35° to the South. The projected image emphasizes the positive (blue) part of the two-lobed pulses seen in raw RFs (Fig. 2a).

2. Petrological evidence

Many basalts from the Central Kamchatka Depression are distinguished from other arc occurrences in having high MgO primitive characteristics. Of the 914 lava samples compiled by Portnyagin et al. (2007), a significant population contains MgO >9%, and these have a wide range of CaO contents. For the low MgO lavas having <9% MgO, clinopyroxene and later plagioclase fractionation are revealed in the positive correlation of MgO and CaO (Fig. 4). However, for the high MgO lavas, clinopyroxene addition and subtraction could not have been the dominant process controlling CaO. Derivative magmas produced by clinopyroxene fractionation from a high MgO and CaO primary magma will not only have low contents of CaO, but they will also be low in SiO₂. This is in contrast to observed high MgO lavas that contain both low CaO and high SiO₂. Therefore, some other process is controlling the substantial

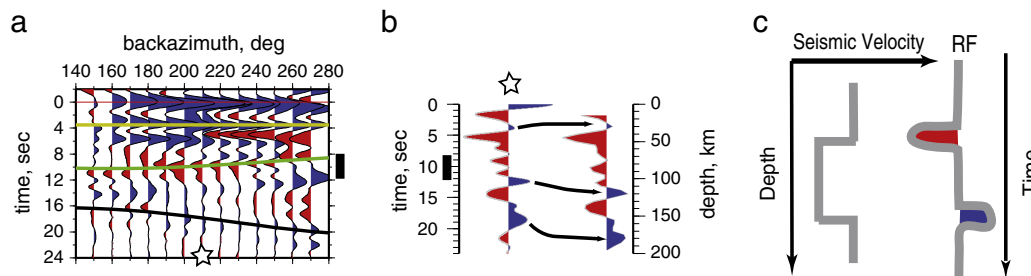


Fig. 2. Steps in constructing, and interpreting, an image of velocity distribution on the basis of receiver function time series. a) Receiver functions arranged by back azimuth. Each trace is averaged over all epicentral distances. Colored lines represent expected arrival times from the crust–mantle boundary at 30 km, an interface at 100 km depth dipping 35° to the south, and an interface at 200 km depth dipping 35° in the direction of Pacific Plate subduction (310°). Black bar marks the sequence of pulses (first negative then positive) that follow the trend expected for a dipping interface at 100 km; b) A single “beam” RF (back azimuth 240°, epicentral distance 80°; star in (a) marks its location) is presented in its original form on the left, and in a depth-projected form on the right. Black arrows show how different elements of the original time series map into depth; c) a cartoon illustrating the logic of interpreting RF pulses (e.g., those marked by black bar in a) and b)) – positive (blue) pulses signify a velocity increase with depth, negative – a decrease. (For interpretation of the references to color in this figure legend, the reader is referred to the web version of this article.)

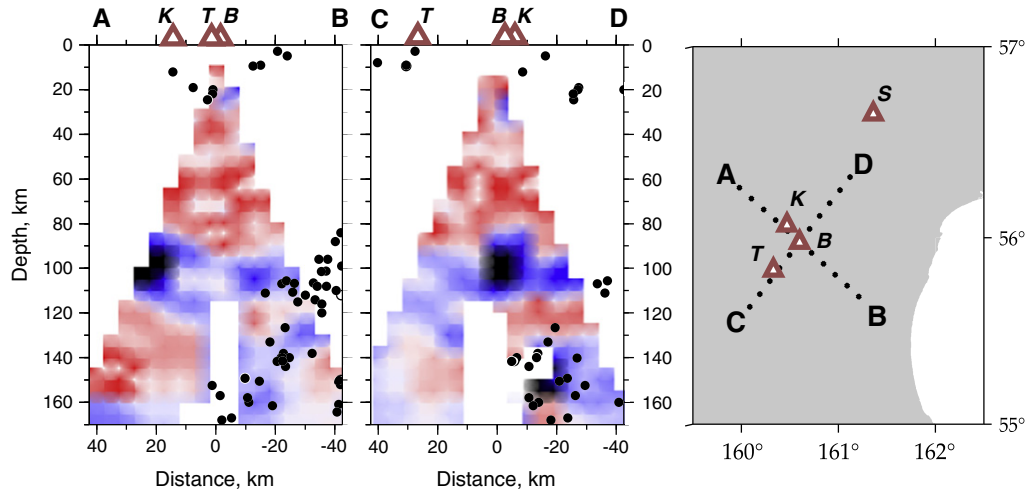


Fig. 3. Migrated RF profile images, showing the location of the upper mantle anomaly. Right panel shows profile orientations. Black circles indicate hypocenters of local earthquakes within 20 km of the profile. Letters indicate volcano names (K – Klyuchevskoy, T – Tolbachik, B – Bezmianny, S – Shiveluch).

major element variability, and Portnyagin et al. (2007) suggested a role for pyroxenite.

High MgO lavas have been separated into high and low CaO populations defined by the broken line in Fig. 4. Primary magmas of anhydrous mantle peridotite have high CaO contents (Herzberg, 2006; Herzberg and Asimow, 2008), and recent experiments with water show that CaO remains high (Balta, personal communication). We therefore infer that lavas from the CKD with high CaO contents melted from a peridotite source, and these are found at the Tolbachik volcano. Lavas from the shield building volcanoes of Hawaii plot below the broken line in Fig. 4 (Herzberg, 2006, 2011), and a role for pyroxenite melting has been suggested (Herzberg, 2011; Sobolev et al., 2007). Similarly, we infer that low contents of CaO in CKD lavas is an indicator of pyroxenite melting, and this is revealed in lavas from the active Tolbachik, Klyuchevskoy and Shiveluch volcanoes, extinct Zarechny and Kharchinsky volcanoes between them, and Shisheisky complex to the north of Shiveluch. There is also a northward decrease in CaO contents of CKD lavas (Fig. 5), indicating

a more prominent role for pyroxenite melting to the north. Portnyagin et al. (2009) similarly inferred a greater participation of pyroxenite northward based on lower Ca contents of olivine phenocrysts to the north. Our conclusions regarding the importance of pyroxenite melting from whole rock CaO contents (Fig. 4) are in good agreement with pyroxenite inferred from high precision olivine phenocryst data (Portnyagin et al., 2009).

3. Discussion

In the Nikulin et al. (2010) study we referred to the observed low velocity feature beneath the KG as the Klyuchevskoy Upper Mantle Anomaly (KUMA). Results of RF migration of a larger dataset presented here serve as further evidence for the presence of this feature in the upper mantle. Details of the observed RFs are shown in Fig. 2a. The sequence of pulses at 9–14 s delay were interpreted in Nikulin et al. (2010) as evidence for a sharply bounded low-velocity layer in the upper mantle. Sharpness of the boundaries was inferred from the relatively high frequency of the pulses, while their order (first

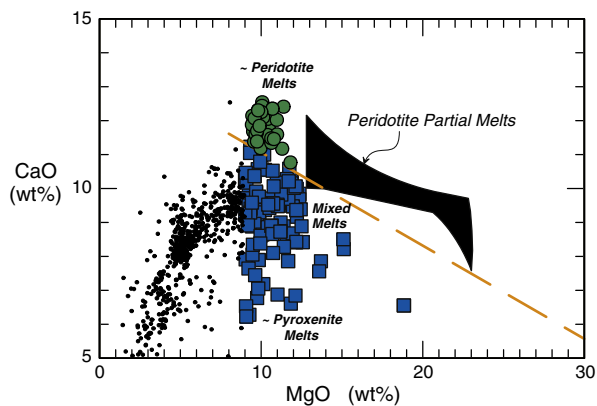


Fig. 4. MgO and CaO contents of lavas from the Central Kamchatka Depression (Portnyagin et al., 2007). Black form shows partial melts of anhydrous peridotite produced by accumulated fractional melting (adapted from Herzberg and Asimow, 2008). Broken line separates partial melts of peridotite above from pyroxenite partial melts below (Herzberg and Asimow, 2008). Green circles show primitive high MgO lavas that originated from a dominant peridotite source lithology, blue squares – high MgO (>9 wt.%) lavas that originated with a mixed peridotite and pyroxenite source provenance (Portnyagin et al., 2009). Small black circles are lavas that exhibit crustal fractional crystallization of plagioclase and clinopyroxene. (For interpretation of the references to color in this figure legend, the reader is referred to the web version of this article.)

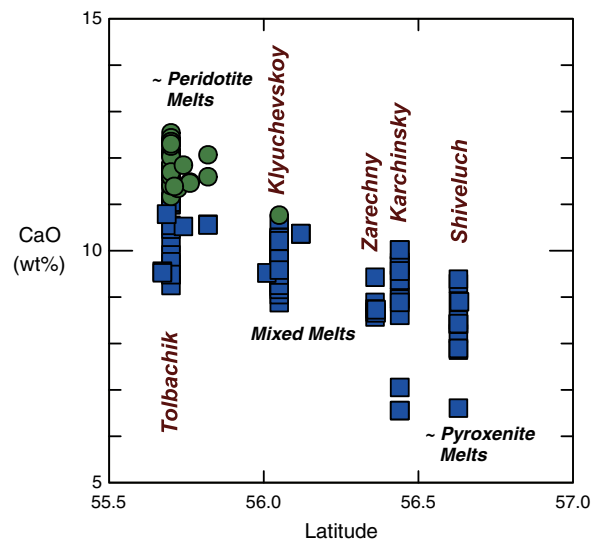


Fig. 5. The variation of CaO in high MgO primitive lavas with latitude (Portnyagin et al., 2007). Lava compositions and their symbols are the same as those in Fig. 4. Primitive low CaO pyroxenite mantle melts become increasingly common to the north.

negative, then positive) was taken as evidence of the low velocity layer. Fig. 2c illustrates the link between pulse polarity and the sign of velocity change with depth.

Nikulin et al. (2010) discussed a number of previously proposed geodynamic scenarios that could create a low velocity layer in the upper mantle beneath the KG, such as a 3D flow of the mantle material around the corner of the subducting Pacific Plate, a sinking lithospheric fragment left behind by subduction zone rearrangement, and a plume of sediments from the subducting Pacific Plate. A contribution of hot asthenosphere mantle flow around the truncated edge of the Pacific slab (Park et al., 2002; Peyton et al., 2001) is effectively ruled out by the sharp (~2 km, Nikulin et al. (2010)) velocity contrast implied for KUMA. Instead, observations suggest a boundary that is caused dominantly by an abrupt change in material properties, and not temperature. The presence of a remnant lithospheric fragment in the mantle wedge, as proposed by Avdeiko et al. (2007), is geodynamically difficult; it is unclear how a relatively large fragment of oceanic lithosphere could remain suspended for a prolonged period of time. A plume of sediments, either rising from the depth ~200 km (Gerya and Yuen, 2003) or else propagating into the mantle wedge laterally (Currie et al., 2007) could help explain the low velocities inferred for KUMA feature, but geochemical evidence of sediment-derived melts in the KG lavas is lacking (Kersting and Arculus, 1995).

Recently, Auer et al. (2009) proposed a scenario in which H₂O enriched fluid is driven from subducted oceanic crust to interact with previously hydrated lithospheric material in the mantle wedge beneath the KG, resulting in a highly productive melt regime. Authors argue for a pre-existing source of high $\delta^{18}\text{O}$ peridotitic magma beneath the KG to explain the high productivity, high $\delta^{18}\text{O}$ and H₂O values observed in the KG lavas. They propose that the subduction episode that formed the SR (Fig. 1) would have hydrated the upper mantle. A subsequent shutdown of that subduction zone and the migration of the trench to its present position would produce a system where primitive basaltic melts rising within the contemporary peridotitic mantle wedge ascend, interact and

assimilate higher- $\delta^{18}\text{O}$ peridotite in the previously heavily hydrated uppermost mantle. Presence of fluid-enriched and potentially partially molten mantle material would, in fact, result in a significant decrease of seismic velocities and strong converted waves observed in our data, if there was a mechanism to concentrate them into a planar body. This process does not, however, explain the signature of pyroxenite melting and its variation with position within the CKD (Figs. 4, 5).

If we assume that low velocities in the upper mantle seismic anomaly and the signature of pyroxenite melting arise from the same source, two geodynamic scenarios appear plausible. The sharp boundaries and planar geometry of the seismic anomaly are consistent with it representing the crustal portion of a detached fragment of oceanic lithosphere, while pyroxenite signature will arise when eclogitized part of the crustal material will melt. As discussed above, such a fragment is unlikely to remain suspended in the asthenosphere, and acceptance of this scenario implies that we are observing a highly transient set of conditions. Support for the transient nature of the KG volcanism may be found in its relative youth, and remarkable vigor.

Another possibility is that the low seismic speed layer represents a zone of concentration for a “second-stage” pyroxenite formed via fluid-rock reaction. We can envisage a SiO₂-rich fluid originating from the subducted slab at ~170 km depth reacting with peridotite in the overlying wedge to produce an orthopyroxene-rich pyroxenite (Fig. 6). This pyroxenite may begin to form close to the slab in vertical rising filaments, and will eventually self-organize into a layer at ~100 km depth, possibly due to the neutral density with respect to the ambient mantle peridotite. As the primitive CKD lavas are mixtures of the melts from peridotite and pyroxenite sources (Portnyagin et al., 2009), the greater contribution of pyroxenite melting to the north would be consistent with this low velocity layer shallowing to the north, as implied by our seismic observations. The formation of the pyroxenite melt rich layer may be related to the geometry and state of the mantle wedge beneath CKD. The upper mantle here is characterized by very low seismic wave speeds

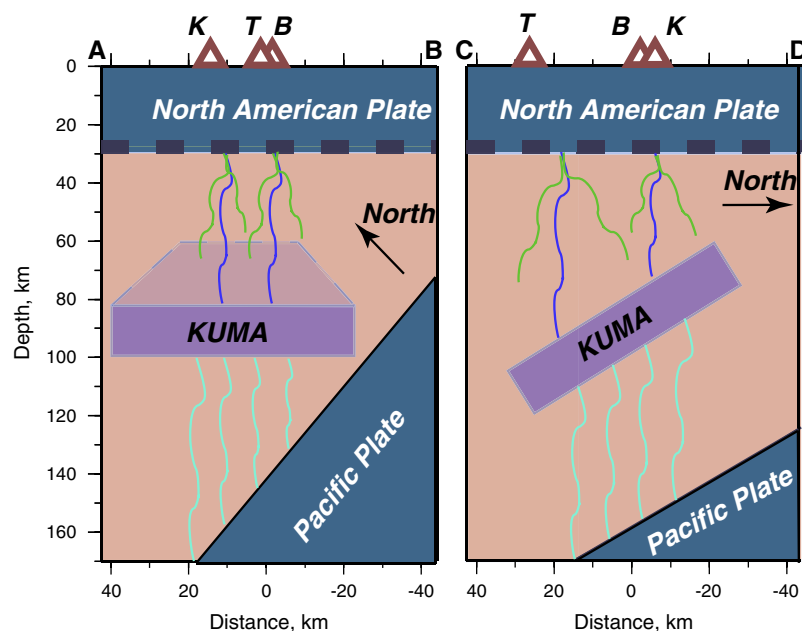


Fig. 6. A schematic presentation of geophysical and petrological observations. Cross-sections are in the same orientation as in Fig. 3. Light blue lines ascending from the subducting Pacific Plate indicate high-H₂O fluid flux. KUMA (purple rectangle) is the proposed concentration of pyroxenite and its melts, labeled as dark blue lines. Green lines indicate peridotite melts. Both melt types undergo mixing prior to eruption at CKD volcanoes. (For interpretation of the references to color in this figure legend, the reader is referred to the web version of this article.)

(Levin et al., 2002), suggesting that the “lithospheric mantle” is likely missing. Thus the path for slab-derived melts from the very deep Pacific slab is unusually long.

We find the second-stage pyroxenite melts scenario particularly appealing. It offers a way to explain both geophysical and geochemical data we presented with a process that does not depend on a set of unique tectonic circumstances. Rather, it offers a possible pathway to forming pyroxenite-derived lavas in other subduction zones with very deep slabs.

Acknowledgments

This research evolved from the work AN performed in the framework of the US–Russia PIRE program, and also made use of the public geochemical database GEOROC. Reviews by an anonymous reviewer and by Maxim Portnyagin helped us formulate our ideas better. We are especially indebted to Dr. Portnyagin for his timely contribution of the geochemical database that supersedes GEOROC. AN was supported by the grant from the Rutgers University Graduate School – New Brunswick. Additional support for this work came from NSF grant EAR 1015422. Figures were drafted using GeoMapApp and GMT software packages.

References

- Ariskin, A.A., Barmina, G.S., Ozerov, A.Yu., Nielsen, R.L., 1995. Genesis of high-alumina basalts from Klyuchevskoy volcano. *Petrology* 3 (5), 449–472. Translated from *Petrologiya*, Vol. 3, No. 5, 1995, 496–521.
- Auer, S., Bindeman, I., Wallace, P., Ponomareva, V., Portnyagin, M., 2009. The origin of hydrous, high- $\delta^{18}\text{O}$ voluminous volcanism: diverse oxygen isotope values and high magmatic water contents within the volcanic record of Klyuchevskoy volcano, Kamchatka, Russia. *Contrib. Mineral. Petrol.* 157, 209–230.
- Avdeiko, G.P., Savelyev, D.P., Palueva, A.A., Popruzhenko, S.V., 2007. Evolution of the Kurile–Kamchatkan Volcanic Arcs and dynamics of the Kamchatka–Aleutian junction. *Volcanism and Subduction: The Kamchatka Region: Geophysical Monograph Series*, 172, pp. 37–55.
- Balesta, S.T., Farberov, A.I., Smirnov, V.S., Tarakanovsky, A.A., Zubin, M.I., 1977. Deep crustal structure of the Kamchatkan volcanic regions. *Bull. Volcanol.* 40, 260–266.
- Bostock, M.G., 1999. Seismic waves converted from velocity gradient anomalies in the Earth's upper mantle. *Geophys. J. Int.* 138, 747–756.
- Braitseva, O.A., Melekestsev, I.V., Ponomareva, V.V., Sulerzhitsky, L.D., 1995. The ages of calderas, large explosive craters and active volcanoes in the Kuril–Kamchatka region. *Bull. Volcanol.* 57, 383–402.
- Crotwell, H.P., Owens, T.J., Ritsema, J., 1999. The TauP Toolkit: flexible seismic travel-time and ray-path utilities. *Seismol. Res. Lett.* 70, 154–160.
- Currie, C.A., Beaumont, C., Huismans, R.S., 2007. The fate of subducted sediments: a case for backarc intrusion and underplating. *Geology* 35, 1111–1114.
- Dorendorf, F., Wiechert, U., Wörner, G., 2000. Hydrated sub-arc mantle: a source for the Klyuchevskoy volcano, Kamchatka/Russia. *Earth Planet. Sci. Lett.* 175, 69–86.
- Fedotov, S.A., Khrenov, A.P., Jarinov, N.A., 1987. Klyuchevskoy volcano, its activity in 1932–1986 and possible development. *Volcanol. Seismol.* 4, 3–16.
- Ferris, A., Abers, G.A., Christensen, D.H., Veenstra, E., 2003. High resolution image of the subducted Pacific (?) Plate beneath central Alaska. *Earth Planet. Sci. Lett.* 214 (3–4), 575–588.
- Gerya, T.V., Yuen, D.A., 2003. Rayleigh–Taylor instabilities from hydration and melting propel “cold plumes” at subduction zones. *Earth Planet. Sci. Lett.* 212, 47–62.
- Gill, J., 1981. *Orogenic Andesites and Plate Tectonics*. Springer, New York.
- Gorbatov, A., Kostoglodov, V., Gerardo, S., Gordeev, E., 1997. Seismicity and structure of the Kamchatka subduction zone. *J. Geophys. Res.* 102, 17883–17898.
- Herzberg, C., 2006. Petrology and thermal structure of the Hawaiian plume from Mauna Kea volcano. *Nature* 444, 605–609.
- Herzberg, C., 2011. Identification of source lithology in the Hawaiian and Canary Islands: implications for origins. *J. Petrol.* 52, 113–146. *Geochemistry, Geophysics, Geosystems* 8, Q09001. doi:10.1029/2008GC002057.
- Herzberg, C., Asimow, P.D., 2008. Petrology of some oceanic island basalts: PRIMELT2.XLS software for primary magma calculation. *Geochem. Geophys. Geosyst.* 8, Q09001. doi:10.1029/2008GC002057.
- Ishikawa, T., Tera, F., Nakazawa, T., 2001. Boron isotope and trace element systematics of the three volcanic zones in the Kamchatka arc. *Geochem. Cosmochim. Acta* 65, 4523–4537.
- Kennett, B.L.N., Engdahl, E.R., Bul, R., 1995. Constraints on seismic velocities in the Earth from travel times. *Geophys. J. Int.* 122, 108–124.
- Kersting, A.B., Arculus, R.J., 1994. Klyuchevskoy volcano, Kamchatka, Russia: the role of high-flux recharged, tapped, and fractionated magma chamber(s) in the genesis of high- Al_2O_3 from high-MgO basalt. *J. Petrol.* 35, 1–41.
- Kersting, A.B., Arculus, R.J., 1995. Pb isotope composition of Klyuchevskoy volcano, Kamchatka and north Pacific sediments: implications for magma genesis and crustal recycling in the Kamchatkan arc. *Earth Planet. Sci. Lett.* 136, 133–148.
- Khubunaya, S.A., Bogoyavlenskiy, S.O., Novogorodtseva, T.Y., Okrugina, A.I., 1994. The mineralogy of the Klyuchevskoi magnesian basalts depicting the fractionation in the magma chamber. *Volcanol. Seismol.* 15, 315–338.
- Khubunaya, S.A., Gontovaya, L.I., Sobolev, A.V., Niskous, I., 2007. Magma chambers beneath Klyuchevskoy group volcanoes. *Volcanol. Seismol.* 2, 32–54.
- Langston, C.A., 1981. Evidence for the subducting lithosphere under southern Vancouver Island and western Oregon from teleseismic P-wave conversions. *J. Geophys. Res.* 86, 3857–3866.
- Levin, V., Shapiro, N., Park, J., Ritzwoller, M., 2002. Seismic evidence for catastrophic slab loss beneath Kamchatka. *Nature* 418, 763–767.
- Nikulin, A., Levin, V., Park, J., 2009. Receiver function study of the Cascadia megathrust: evidence for localized serpentinization. *Geochem. Geophys. Geosyst.* 10, Q07004. doi:10.1029/2009GC002376.
- Nikulin, A., Levin, V., Shuler, A., West, M., 2010. Anomalous seismic structure beneath the Klyuchevskoy Group, Kamchatka. *Geophys. Res. Lett.* 37, L14311. doi:10.1029/2010GL043904.
- Nizkous, I.V., Sanina, I.A., Kissling, E., Gontovaya, L.I., 2006. Velocity properties of the lithosphere in the ocean-continent transition zone in the Kamchatka region from seismic tomography data. *Izvestiya. Phys. Solid Earth* 42, 286–296.
- Ozerov, A.Y., 2000. The evolution of high-alumina basalts of the Klyuchevskoy Volcano, Kamchatka, Russia, based on microprobe analyses of mineral inclusions. *J. Volcanol. Geotherm. Res.* 95, 65–79.
- Park, J., Levin, V., 2000. Receiver functions from multiple-taper spectral correlation estimates. *Bull. Seismol. Soc. Am.* 90, 1507–1520.
- Park, J., Levin, V., Brandon, M., Lees, J., Peyton, V., Gordeev, E., Ozerov, A., 2002. A dangling slab, amplified arc volcanism, mantle flow, and seismic anisotropy in the Kamchatka plate corner. In: Stein, S., Freymueller, J. (Eds.), *Plate Boundary Zones: AGU Geodynamics Series*, v. 30, pp. 295–324.
- Park, J., Yuan, H., Levin, V., 2004. Subduction-zone anisotropy under Corvallis, Oregon: a serpentinite skidmark of trench-parallel terrane migration? *J. Geophys. Res.* 109, B10306. doi:10.1029/2003JB002718.
- Peyton, V., Levin, V., Park, J., Brandon, M., Lees, J., Gordeev, E., Ozerov, A., 2001. Mantle flow at a slab edge: seismic anisotropy in the Kamchatka region. *Geophys. Res. Lett.* 28, 379–382.
- Phinney, R.A., 1964. Structure of the Earth's crust from spectral behavior of long-period body waves. *J. Geophys. Res.* 69, 2997–3017.
- Portnyagin, M., Manea, V.C., 2008. Mantle temperature control on composition of arc magmas along the Central Kamchatka Depression. *Geology* 36 (7), 519–522.
- Portnyagin, M., Bindeman, I., Hoernle, K., Hauff, F., 2007. Geochemistry of primitive lavas of the Central Kamchatka Depression: magma generation at the edge of the Pacific plate. *AGU Geophys. Monogr.* 172, 203–244.
- Portnyagin, M.V., Sobolev, A.V., Mironov, N.L., Hoernle, K., 2009. Pyroxenite melts involved in magma genesis in Kamchatka. 19th Annual V.M. Goldschmidt Conference, Davos, Switzerland, June 21–26. *Geochim. Cosmochim. Acta* 73, A1044.
- Shapiro, N.M., Gorbatov, A.V., Gordeev, E., Dominguez, J., 2000. Average shear-velocity structure of the Kamchatka peninsula from the dispersion of surface waves. *Earth Planets Space* 52, 573–577.
- Sobolev, A.V., Hofmann, A.W., Kuzmin, D.V., Yaxley, G.M., Arndt, N.T., Chung, S.-L., Danyushevsky, L.V., Elliott, T., Frey, F.A., Garcia, M.O., Gurenko, A.A., Kamenetsky, V.S., Kerr, A.C., Krivolutskaya, N.A., Matvienkov, V.V., Nikogosian, I.K., Rocholl, A., Sigurdsson, I.A., Sushchevskaya, N.M., Teklay, M., 2007. The amount of recycled crust in sources of mantle-derived melts. *Science* 316, 412–417.
- Syracuse, E.M., Abers, G.A., 2006. Global compilation of variations in slab depth beneath arc volcanoes and implications. *Geochem. Geophys. Geosyst.* 7, Q05017. doi:10.1029/2005GC001045.
- Tatsumi, Y., 1986. Formation of the volcanic front in subduction zones. *Geophys. Res. Lett.* 13 (8), 717–720.
- Tatsumi, W., Eggins, S., 1995. *Subduction Zone Magmatism*. Blackwell Sci., Malden, Mass.
- Vinnik, L.P., 1977. Detection of waves converted from P to SV in the mantle. *Phys. Earth Planet. Int.* 15, 39–45.
- Volynets, O.N., 1994. Geochemical types, petrology and genesis of Late Cenozoic volcanic rocks from the Kurile–Kamchatka island-arc system. *Int. Geol. Rev.* 36, 373–405.
- Yogodzinski, G.M., Lees, J.M., Churikova, T.G., Dorendorf, F., Woerner, G., Volynets, O.N., 2001. Geochemical evidence for the melting of subducting oceanic lithosphere at plate edges. *Nature* 409, 500–504.